Technical Note

Interference Mitigation using a Dual-Polarized Antenna: a deep analysis in Space domain and Polarimetric domain

Matteo Sgammini

German Aerospace Center (DLR), Oberpfaffenhofen, 82234 Wessling, Germany, e-mail:

Matteo.sgammini@dlr.de, phone: +49-8153-28-2375, fax: +49-8153-28-2328 (corresponding author)

Reference paper: *M. Sgammini et al., "Interference Mitigation Using a Dual-Polarized Antenna in a Real Environment, " in Proc. of the 29th Int. Technical Meeting of the Satellite Division of The Institute of Navigation (ION GNSS+ 2016), Portland, OR, September 2016.*

In this work we aim at providing a comprehensive understanding of the behaviour of a Dual-polarized (DP) array in both space and polarimetric domains.

To this intent the CW interference scenario illustrated in Figure 1 has been considered, in view of the circumstance that the DoA of PRN22 and PRN14 almost coincide with the DoA of the CW interferer, as illustrated in the sky plot in Figure 2.

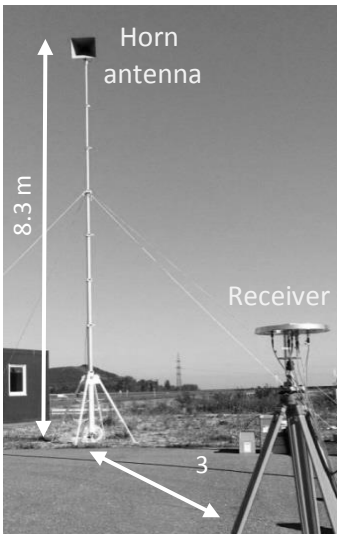

Figure 1 - CW interference scenario

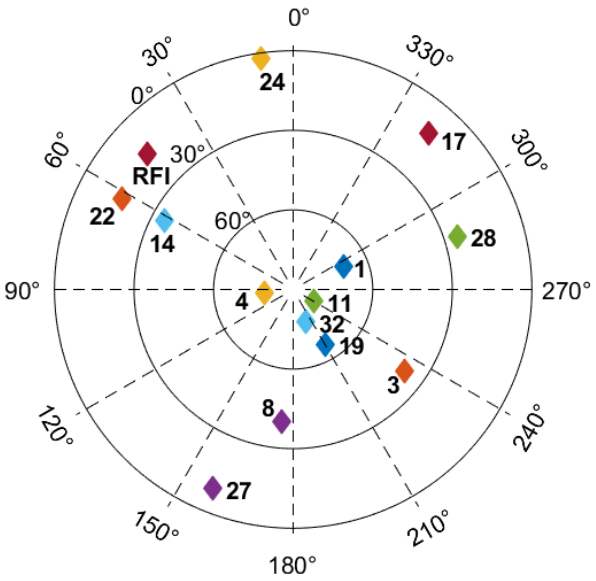

Figure 2 - Receiver sky plot for GPS L1 on October 22th, 2015, at 13:10:00 UTC

It must be noted that the results shown in this work are obtained using the antenna characterization measured in an anechoic camber. This can sensibly differ from the operational antenna response when employed in the field, in particular wrong assumption on antenna array manifold are most likely at low elevation angles and with regard to the cross-polar components, in literature this condition is referred as manifold mismatch.

As pointed out in [1], the key concept of a DP array is the possibility to discriminate in polarimetric domain. We want now to exhibit this feature by means of 2-D representations in the polarimetric domain. First of all let estimate the polarization of the incident CW interference and of an exemplary satellite signal under interference-free

condition, the PRN22 in this case. Figure 3 shows these results using a MUSIC search algorithm spanning the polarization space, i.e. for any value of the polarization coefficients ϵ_x, ϵ_y and ϕ, which corresponds varying $\boldsymbol{k} = [\epsilon^R, \epsilon^L]^T$ in

$$\begin{aligned} \boldsymbol{v}^R(\psi, \epsilon^R, \epsilon^L, t) &= (\boldsymbol{a}^{RC}(\psi)\epsilon^R + \boldsymbol{a}^{RX}(\psi)\epsilon^L)\,\rho(t-\tau) \\ &= \boldsymbol{b}^R(\psi, \epsilon^R, \epsilon^L)\rho(t-\tau) \\ \boldsymbol{v}^L(\psi, \epsilon^R, \epsilon^L, t) &= (\boldsymbol{a}^{LX}(\psi)\epsilon^R + \boldsymbol{a}^{LC}(\psi)\epsilon^L)\,\rho(t-\tau) \\ &= \boldsymbol{b}^L(\psi, \epsilon^R, \epsilon^L)\rho(t-\tau) \end{aligned} \quad (1)$$

following the linear to circular basis conversion:

$$\begin{aligned} \boldsymbol{e} &= \left(\frac{1}{\sqrt{2}}(\epsilon_x - i\epsilon_y e^{i\phi})\hat{\boldsymbol{e}}^R + \frac{1}{\sqrt{2}}(\epsilon_x + i\epsilon_y e^{i\phi})\hat{\boldsymbol{e}}^L\right)e^{i\phi_x} \\ &= (\epsilon_r\,\hat{\boldsymbol{e}}^R + \epsilon_l\,\hat{\boldsymbol{e}}^L)e^{i\phi_x} \equiv \begin{bmatrix}\epsilon^R \\ \epsilon^L\end{bmatrix} e^{i\phi_x} \end{aligned} \quad (2)$$

Note that a polarimetric MUSIC algorithm searching jointly in space and polarimetric domain can be applied to estimate signal polarization as described in [2] and [3], however we are not merely interested to know the polarization of an incident signal, but rather to understand the behaviour of the system in the polarimetric space. For this purpose we define the MUSIC spectrum as

$$S_{MUSIC}(\boldsymbol{k}) = \left[\frac{\boldsymbol{k}^H\tilde{\boldsymbol{a}}^H(\hat{\psi})\,\boldsymbol{U}_N\boldsymbol{U}_N^H\,\tilde{\boldsymbol{a}}(\hat{\psi})\,\boldsymbol{k}}{\boldsymbol{k}^H\tilde{\boldsymbol{a}}^H(\hat{\psi})\,\boldsymbol{k}}\right]^{-1} \quad (3)$$

where $\tilde{\boldsymbol{a}} = \begin{bmatrix}\tilde{\boldsymbol{a}}^R(\hat{\psi}) \\ \tilde{\boldsymbol{a}}^L(\hat{\psi})\end{bmatrix} = \begin{bmatrix}\tilde{\boldsymbol{a}}^{RC}(\hat{\psi}) & \tilde{\boldsymbol{a}}^{RX}(\hat{\psi}) \\ \tilde{\boldsymbol{a}}^{LX}(\hat{\psi}) & \tilde{\boldsymbol{a}}^{LC}(\hat{\psi})\end{bmatrix}$, $\tilde{\boldsymbol{a}}$ indicates the measured antenna responses, and $\hat{\psi}$ is the DoA estimate of the polarimetric MUSIC for either the LOS or the RFI signal.

To facilitate the reader the figures include marks indicating the position of principal polarizations, that is a green cross for a pure RHCP, a light blue cross for a pure LHCP, a dark gray line for a linear polarization with positive slope and a light gray line for a linear polarization with negative slope. The MUSIC algorithm searches for vectors having the minimum projection into the noise subspace spanned by $\mathrm{R_{nn}}$. The outcome presented in Figure 3(a) evinces the signal present at pre-correlation stage, i.e. the CW interference, to be linearly polarized with positive slope and tilt angle of about 60 deg. The result matches the expectation of a linearly polarized wave emitted by the

horn antenna. Figure 3(b) shows the MUSIC spectrum when searching for the signal polarization of PRN22 under interference-free condition, as expected it clearly indicates a RHCP polarized signal.

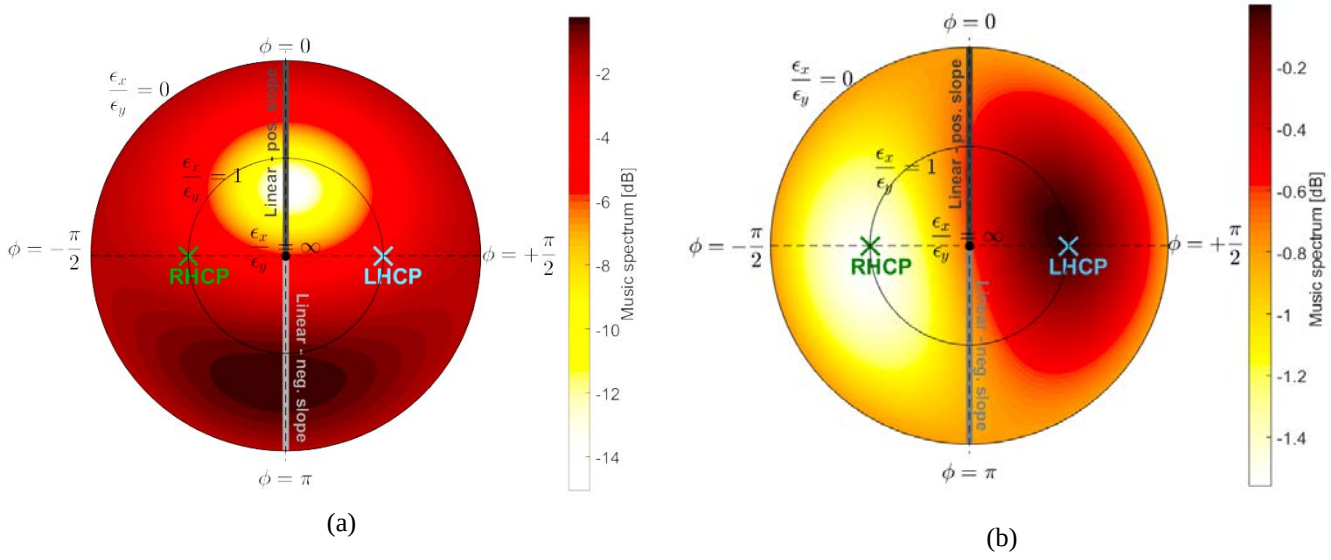

Figure 3 - MUSIC spectrum in polarization domain
(a) At pre-correlation stage in presence of the CW interference, (b) At post-correlation for PRN22 under interference-free condition

A meaningful figure of merit to assess the performance of the antenna array is the realized array gain, which is the power gain the received signal experience when passing through the antenna and the blind beamformer. It depends on both polarization and DoA. Due to various sources of errors that arise in the practice, like the manifold mismatch discussed above, the antenna gain is only an estimate of the real antenna gain, and it can be obtain by fixing either the polarization ϵ^R and ϵ^L or the DoA ψ of the observed signal. Figure 4(a) shows the array gain for PRN22 under interference-free condition in polarization domain for a fixed $\widehat{\psi}_{\mathrm{PRN}_{22}}$, where $\widehat{\psi}_{\mathrm{PRN}_{22}}$ is the DoA estimation outcome of the conventional MUSIC. The estimate of the gain of PRN22, assumed as a pure RHCP signal, indicates an improvement of about 1 dB, and a deep null for any LHCP components, such as multipath.

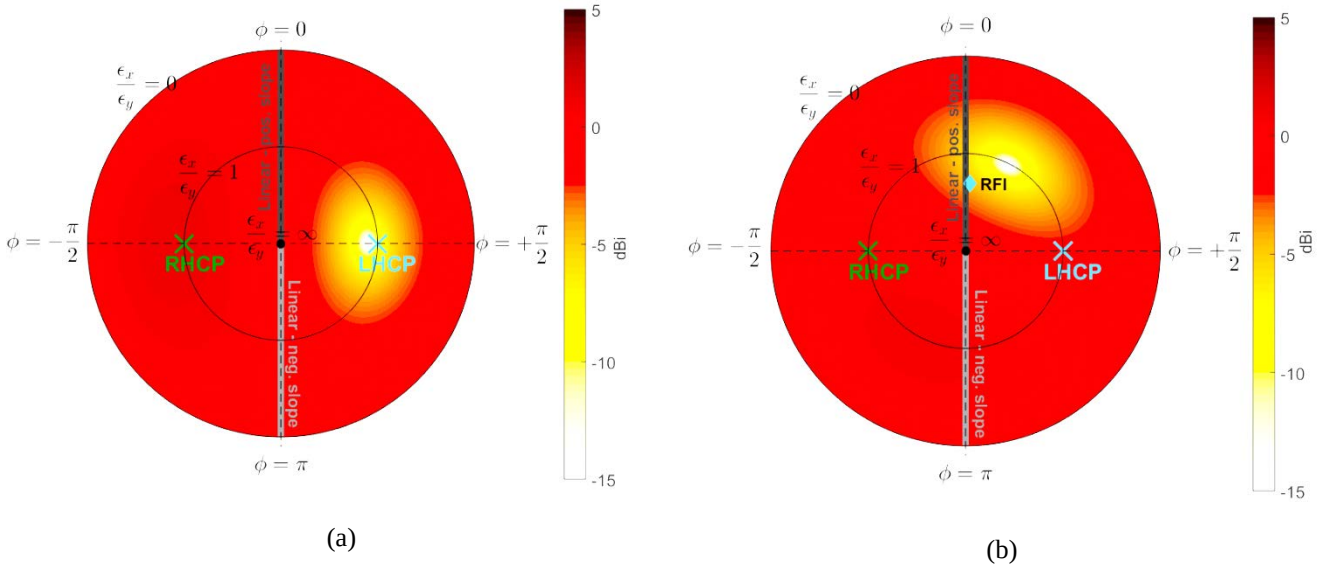

Figure 4 - Antenna gain after two-step blind beamforming
(a) PRN22 under interference-free condition, (b) PRN22 in presence of the CW interference

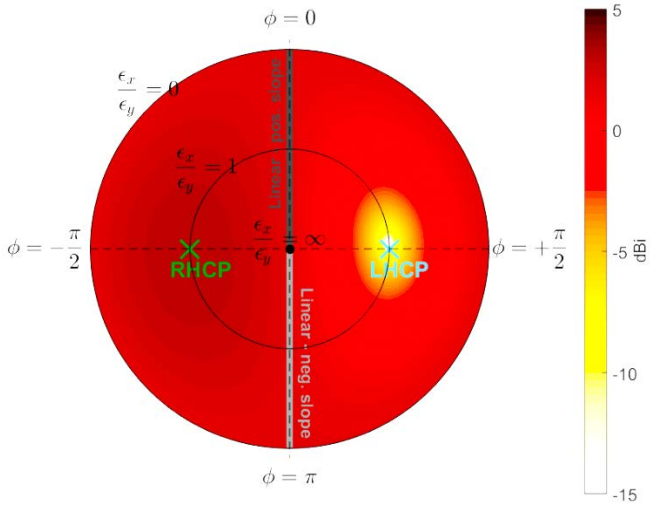

Figure 5 - Antenna gain after two-step blind beamforming for PRN8 in presence of CW interference

Figure 4(b) illustrates the array gain when the CW interference is present, since PRN22 and the RFI are spatial close, the beamformer strives to separate the signals in polarimetric domain, indeed the polarimetric null is placed close to the linear polarization plane with positive slope, providing 6 dB mitigation at $\widehat{\Psi}_{\mathrm{RFI}}$ and tilt angle of 60deg. On the other hand a slightly decrease of the RHCP gain at $\widehat{\Psi}_{\mathrm{PRN}_{22}}$ should be taken into account. This is not the case

for satellite signals having a DoA not overlapping with the DoA of the interference, for those signals the array gain in polarization space remains almost unaffected by the presence or not of the interference, as can be seen in Figure 5, where the exemplary case of PRN8 is illustrated. The same results can be observed under a reciprocal point of view, for instance looking at the array gain fixing the signal polarization $\epsilon^{\mathrm{R}}, \epsilon^{\mathrm{L}}$ and spanning over the space variable ψ. Figure 7 illustrates the antenna gain response for pure RHCP signals, in Figure 7(a) the DP antenna steers the beam into the direction of PRN22, interference can be indeed suppressed in polarization domain. On the contrary when the SP array has been used, the array gain places a null at $\widehat{\psi}_{\mathrm{RFI}}$ impairing also the gain at $\widehat{\psi}_{\mathrm{PRN}_{22}}$, as shown in Figure 7(b), causing the loss-of-lock exhibited in Figure 6(a). Despite that, the interference mitigation capability does not experience any improvement and stays at the same level as in the DP case (about 6 dB).

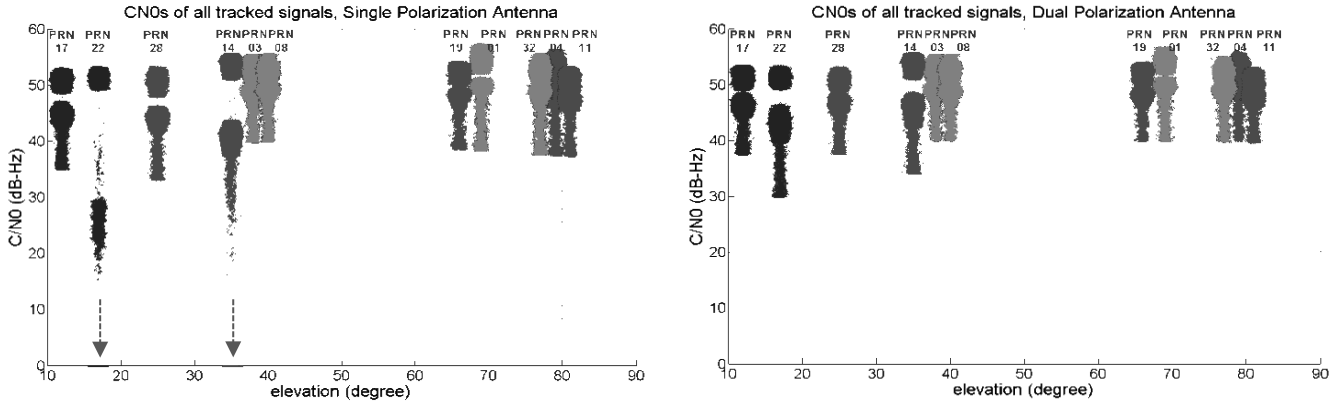

(a) (b)

Figure 6 - C/N_0 history for all the tracked GPS L1 satellites placed in order of their elevation AoA collected over 120sec.
(a) Using the single-polarized antenna, (b) using the dual-polarized antenna

Due to manifold mismatch, caused mainly by wrong assumptions on $\tilde{\boldsymbol{a}}^{Rx}(\widehat{\psi}_{\mathrm{RFI}})$ and $\tilde{\boldsymbol{a}}^{Lx}(\widehat{\psi}_{\mathrm{RFI}})$**,** the deepness of the null at $\widehat{\psi}_{\mathrm{RFI}}$ is strongly compromised, a mitigation value of about 6dB it is in contrast to the power reduction estimate obtained comparing the CW carrier power of $\boldsymbol{X}[k]$ and $\tilde{\boldsymbol{X}}[k]$**,** which indicates a RFI mitigation of at least 60 dB at each of the antenna output.

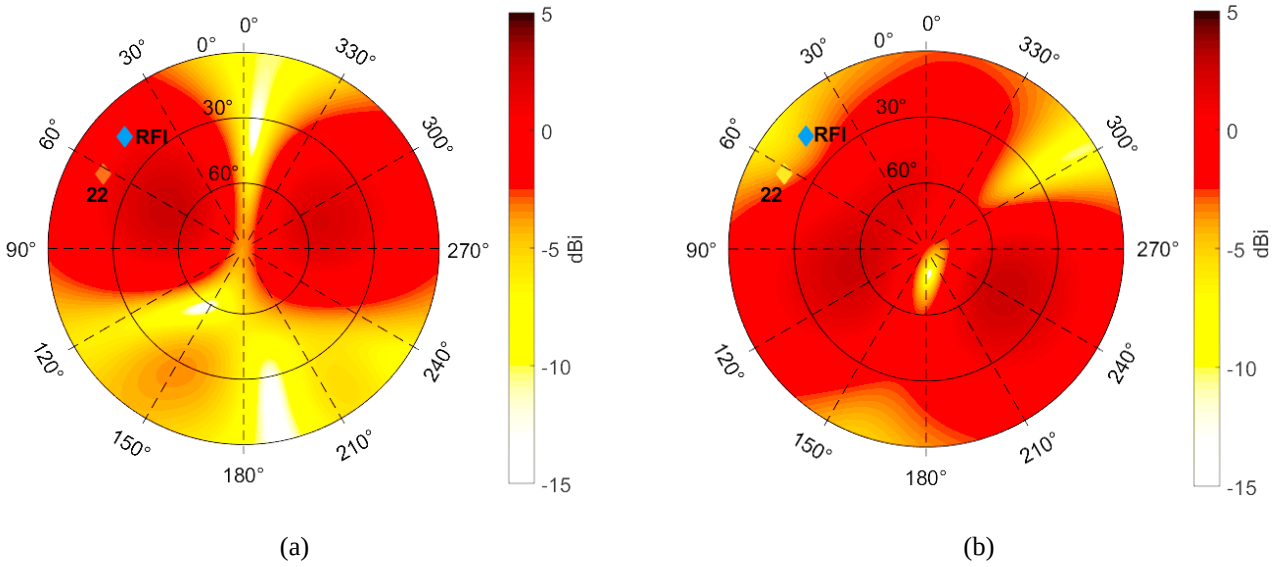

(a) (b)

Figure 7 - RHCP antenna gain after two-step blind beamforming in presence of the CW interference (a) Dual-polarized array, (b) Single-polarized array

[1] M. Sgammini et al., "Interference Mitigation Using a Dual-Polarized Antenna in a Real Environment, " in Proc. of the 29th Int. Technical Meeting of the Satellite Division of The Institute of Navigation (ION GNSS+ 2016), Portland, OR, September 2016.

[2] Ferrara, E., Jr.; Parks, T., "Direction finding with an array of antennas having diverse polarizations," Antennas and Propagation, IEEE Transactions on , vol.31, no.2, pp.231-236, Mar 1983.

[3] R. O. Schmidt, "Multiple emitter location and signal parameter estimation," *IEEE Trans. Antennas Propag.*, vol. 34, no. 3, pp. 276–280, Mar. 1986.